Journal of Materials Chemistry C

Accepted Manuscript

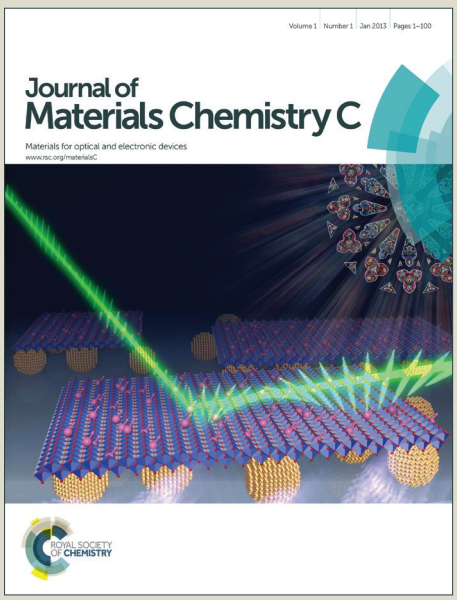

ROYAL SOCIETY OF CHEMISTRY

www.rsc.org/materialsC

Journal of Materials Chemistry C

ARTICLE

Resistive switching in Ga- and Sb-doped ZnO single nanowire devices

Received 10th July 2015,
Accepted 00th January 20xx

DOI: 10.1039/x0xx00000x

www.rsc.org/

Bo Wang,[a] Tianshuang Ren,[a] Si Chen,[a] Bosen Zhang,[a] Rongfang Zhang,[a] Jing Qi,[a,†] Sheng Chu,[b] Jian Huang,[c] Jianlin Liu,[c,†]

Resistive random access memory (RRAM) is one of the most promising nonvolatile memory technologies because of its high potential to replace traditional charge-based memory, which is approaching its scaling limit. To fully realize the potential of the RRAM, it can be important to develop a unique device with current self-rectification, which provides a solution to suppress sneak current in crossbar arrays, and self-compliance, which eliminates current limiter. In this paper, self-rectifying resistive switching is demonstrated in Ga-doped ZnO single nanowire device; the current is not only self-rectifying but also self-compliance for Sb-doped single nanowire devices. Multilevel resistive switching has also been achieved for Sb-doped ZnO single nanowire devices by using different SET voltages. Furthermore, the doping of Ga and Sb narrows the switching voltage distribution greatly.

Introduction

Traditional charge-based memory is approaching its scaling limit. In this circumstance, the development of future nonvolatile memory (NVM) has attracted extensive attention [1]. Resistive random access memory (RRAM) with a simple sandwich structure of metal/insulator/metal (MIM) is one of the emerging NVM technologies. It has superior performance such as faster writing speed, lower operating power, higher endurance, excellent scalability beyond 10 nm feature size using a crossbar structure and multistate memory [2-6] as compared to other counterparts such as phase-change RAM (PRAM), magnetoresistive RAM (MRAM), flash memory and ferroelectric RAM (FeRAM). Resistive switching phenomena are observed in various metal oxides [7, 8], organic molecules [9], polymers [10], graphene oxide [11], and nanocomposites [12]. ZnO is a wide direct-gap II-VI semiconductor, which has abundant oxygen vacancies [13]. This is helpful to the formation of a filamentary conductive path [14]. Resistive switching in ZnO-based devices has been reported [15-20].

To study the scalability of ZnO-based resistive memory, fabrication and characterization of devices with low dimensionality is essential. As one kind of low-dimensional structures, semiconductor nanowires (SNWs) are very useful to achieve various unique functions and/or high-performance electronic and optoelectronic devices due to their intriguing physical and chemical properties, such as rich surface state and large surface area [21, 22], excellent mechanical flexibility [23, 24], resonant light absorption [25, 26], carrier confinement-induced band-gap tunability [27, 28], and so on. Resistive switching phenomena are also observed in all kinds of SNW devices [16, 29-32].

In this paper we report current self-rectifying resistive switching in Ga-doped ZnO single nanowire device, which means that the device has inherent rectifying characteristics at low-resistance state (LRS). We also report current self-rectifying and self-compliance resistive switching in Sb-doped ZnO single nanowire device. Self-compliance characteristics mean that the system itself controls a LRS without needing an external current limiter to protect the device. Current self-rectifying and self-compliance resistive switching can not only provide a solution to suppress sneak current in crossbar arrays [33] but also prevent resistive switching memory from hard breakdown.

Experimental

Ga-doped, Sb-doped, and undoped ZnO nanowires were grown in a quartz tube furnace system. Zinc powder mixed with or without Sb or Ga powder in a quartz bottle was placed in the center of the quartz tube. A Si (100) substrate with 10 nm gold catalyst on top was kept 2 cm away from the source on the downstream side. Nitrogen gas with a flow rate of 1000 sccm passed continuously through the furnace. The source and substrate were then heated to a growth temperature of 540 °C. During the growth, a mixture of argon/oxygen (99.5:0.5) of

[a] The Key Laboratory for Magnetism and Magnetic Materials of MOE, Department of Physics, School of Physical Science and Technology, Lanzhou University, Lanzhou, 730000, China.
[b] School of Physics and Engineering, Sun Yat-sen University, Guang Zhou, 510000, China.
[c] Quantum Structures Laboratory, Department of Electrical and Computer Engineering, University of California, Riverside, California, 92521, USA.
† Corresponding authors: qijing@lzu.edu.cn; jianlin@ece.ucr.edu

300 sccm was introduced to the quartz tube for ZnO nanowire growth. The growth lasted for 30 min. The microstructure of nanowires was evaluated by scanning electron microscopy (SEM). The single-nanowire devices were utilized to evaluate the electrical characteristics, which were fabricated on n-type silicon substrate capped with a thermally oxidized SiO_2 layer of 300 nm. To fabricate the memory device, ZnO nanowires were firstly transferred onto the substrate. Then standard photolithography process was utilized to pattern the substrate with ZnO nanowires on top, followed by deposition of 100 nm Ag. Electrical characterization was performed in air at room temperature with a voltage sweeping rate of **6.4 ms/V** by using semiconductor parameter analyzer (Agilent 4155C).

Results and discussion

Fig.1 (a)-(c) show the SEM images of as-grown undoped, Ga-doped, and Sb-doped ZnO nanowires, respectively. Undoped and Ga-doped ZnO nanowires are well aligned perpendicular to the substrates while Sb-doped ZnO nanowires are randomly oriented. The diameters are estimated to be 50 nm, 100 nm, 100 nm for undoped, Ga-doped and Sb-doped ZnO nanowires, respectively, on average. Fig.1 (d) shows an SEM image of a typical ZnO nanowire device. The distance between two Ag electrodes is about 1μm.

Fig.2 shows energy dispersive X-ray (EDX) log-scale spectra of (a) Ga-doped and (b) Sb-doped ZnO nanowires for the area in the insets of transmission electron microscopy (TEM) images. C and Cu signals are from the TEM holder. Ga and Sb are successfully doped into ZnO nanowires, respectively. The content of Ga and Sb are about 0.39% and 0.71%, respectively.

Fig.3 (a)-(c) show *I-V* characteristics of undoped, Ga-doped, and Sb-doped ZnO single nanowire devices, respectively.

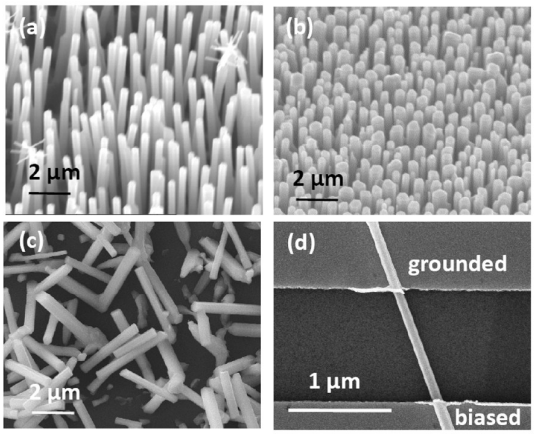

Fig.1 SEM images of (a) undoped, (b) Ga-doped, (c) Sb-doped ZnO nanowires, and (d) typical single ZnO nanowire device. Undoped and Ga-doped ZnO nanowires were grown vertically on the substrates while Sb-doped ZnO nanowires were grown randomly oriented.

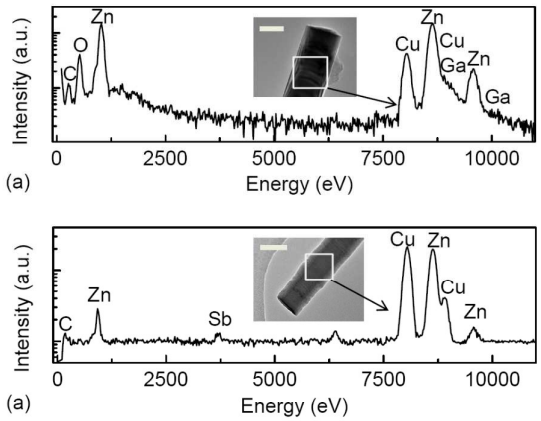

Fig.2 EDX log-scale spectra (insets: TEM images) of (a) Ga-doped, (b) Sb-doped ZnO nanowires. The scale bars in the insets are 100 nm. Ga and Sb are successfully doped into ZnO nanowires, respectively. The content of Ga and Sb are about 0.39% and 0.71%, respectively.

During measurements, one electrode of the device was grounded, for example, top electrode in Fig.1 (d) and the other electrode was biased by DC voltage. The DC voltage was first swept from 0 to 40 V, 0 to -40 V, and 0 to 40 V for undoped, Ga-doped, and Sb-doped ZnO single nanowire devices to carry out electroforming process [34], as shown in the insets of Fig.3 (a), (b), and (c), respectively. Then, the DC voltage was swept following the sequence of 40~0~-40~0~40 V. For undoped ZnO nanowire device, *I-V* characteristics show typical bipolar resistive switching [7]. The RESET and SET voltages are -32 V and 22 V, respectively. The high RESET and SET voltages are caused by the large distance of 1 μm between two electrodes. The high switching voltages are comparable to those of other nanowire resistive switching systems[35, 36]. They are higher than those of resistive system reported in reference 37 because AsS thin film of 100nm is responsible for resistive switching while AAO membrane filled with Ag nanowire only acts as one part of electrode. *I-V* characteristics exhibit self-rectifying bipolar resistive switching behavior [38] for Ga-doped ZnO nanowire device. The forward/reverse current ratio with a -15 V reading voltage at LRS is as large as 130. This property is useful in RRAM based on crossbar structure arrays because the cross talk effect can be restrained and misreading can be avoided [33]. The RESET and SET voltages are 40 V and -25 V respectively. For Sb-doped ZnO single nanowire device, *I-V* characteristics show current self-compliance and self-rectifying resistive switching behavior. If each memory cell in a RRAM circuit has the property of self-complianced and self-rectifying behavior, both current limiter and selector devices are not necessary. Therefore, the circuit fabrication can be greatly simplified and the fabrication cost can be greatly lowered. The self-rectification directions change with the polarity of electroforming process for both Ga-doped and Sb-doped devices. Ga-doped device was negatively electroformed to

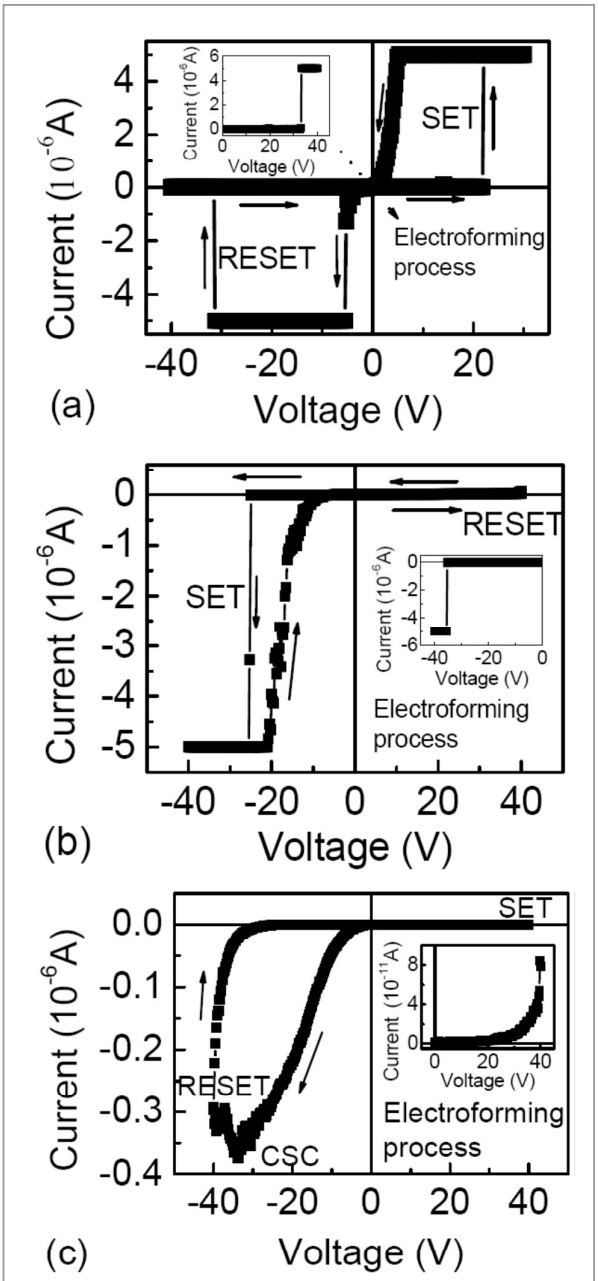

Fig.3 (a)~(c) *I-V* characteristics of (a) undoped, (b) Ga-doped, (c) Sb-doped ZnO single nanowire devices. Insets: *I-V* characteristics of electroforming process for each kind of devices. The undoped ZnO single nanowire device shows typical bipolar RS. The Ga-doped nanowire device shows self-rectified bipolar RS while Sb-doped ZnO single nanowire device shows self-rectified and current-self-complianced bipolar RS.

make sure that the self-rectification directions are the same for Ga-doped and Sb-doped devices. The RESET and SET voltages are -40 V and 40 V, respectively. It is interesting to notice that the RESET voltages are negative for undoped and

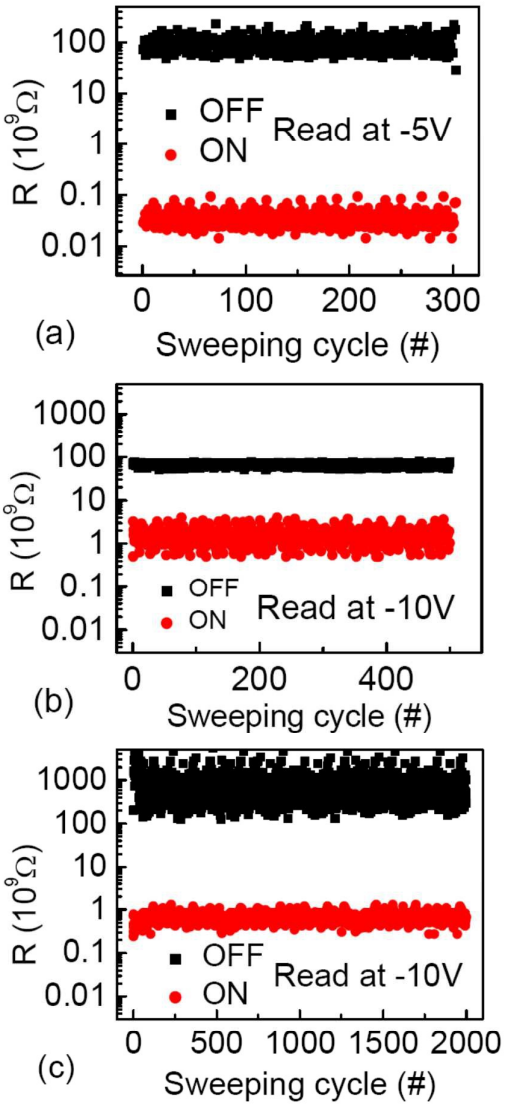

Fig.4 (a)~(c) endurance of (a) undoped, (b) Ga-doped, (c) Sb-doped ZnO single nanowire devices. The DC sweeping endurances of undoped and Ga-doped ZnO devices are about 300 and 500 cycles, respectively, while that of Sb-doped ZnO nanowire device is higher than 2000 cycles.

Sb-doped ZnO single nanowire devices while it is positive for Ga-doped ZnO single nanowire devices. The cause of this polarity change need to be further studied.

Fig.4 (a)-(c) show the endurance characteristics of undoped, Ga-doped, and Sb-doped ZnO single nanowire devices, respectively. The devices were measured in the DC voltage sweeping mode by performing a series of consecutive cycles of 40~0~-40~0~40 V as shown in Fig.3 (a)-(c). The resistances were obtained at -5 V for undoped nanowire devices and at -10 V for doped nanowire devices. The resistances in both states for all three devices are very stable under 300, 500, and 2000 cycles for undoped, Ga-doped, and Sb-doped ZnO single

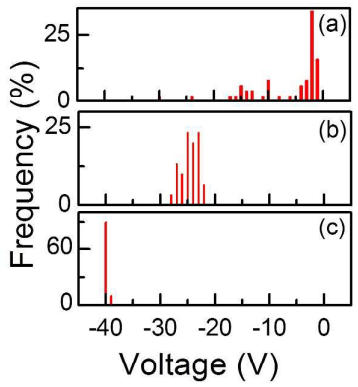

Fig.5 RESET or SET voltage distribution for (a) undoped, (b) Ga-doped, and (c) Sb-doped ZnO single nanowire devices. The RESET voltages distribute between -1 V and -30 V for undoped ZnO single nanowire device. After Ga or Sb doping, the voltage distribution range decreases greatly.

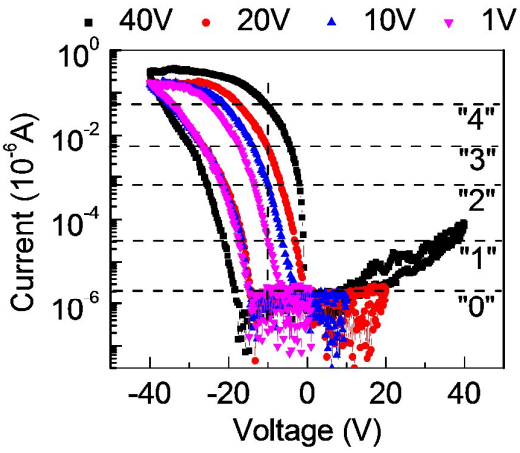

Fig.6 I-V characteristics of Sb-doped ZnO single nanowire device for multilevel memory application by setting at different voltages. By using different SET voltages of 1, 10, 20, and 40 V, the Sb-doped ZnO single nanowire device can be SET at different resistance states, which can be utilized to store different levels such as "0", "1", "2", "3", and "4".

nanowire devices, respectively. After 300 and 500 cycles, respectively, the undoped and Ga-doped nanowire devices were kept at LRS and couldn't be RESET anymore. While after 2000 cycles, the Sb-doped ZnO nanowire devices could still be SET and RESET successfully. The endurance property is relatively poor for undoped device, which is only 300 cycles. With the doping of n-type dopant Ga, the endurance was improved to 500 cycles. While with doping of p-type dopant Sb, it was improved to at least 2000 cycles. 1000 cycles in DC mode can be equivalent to about 10^9 cycles in pulse mode for a 1μs switching time [39].

Fig. 5 (a)-(c) show the statistic distribution of RESET/SET voltages ($V_{SET/RESET}$) during the endurance cycles by DC voltage sweeping for undoped, Ga-doped, and Sb-doped ZnO single nanowire devices, respectively. The $V_{SET/RESET}$ for undoped device is largely fluctuated as -1~-30 V. However, this fluctuation is considerably reduced to -22~-28 V and -39~-40 V in the devices with doping of Ga and Sb, respectively. The cycle-to-cycle uniformity of switching voltages by DC sweep mode was significantly improved by doping of Ga and Sb, esp. Sb.

Fig. 6 shows I-V characteristics of Sb-doped nanowire device under different SET voltages. The HRS current is almost unchanged, while the LRS current decreases with narrowing the voltage sweeping span (V_{max}) from 40 V to 1 V, leading to lower resistance ratio between the LRS and HRS. Specifically, four resistance levels are achieved for LRS by setting V_{max} at 40, 20, 10, and 1 V. As V_{max} is set at 1 V, the current reading at -10 V is about 3×10^{-5} μA, this is designated as level "1". As V_{max} is set at 10, 20, and 40 V, the currents reading at -10 V are about 6×10^{-4}, 6×10^{-3}, and 6×10^{-2} μA, respectively. These states are designated as level "2", "3", and "4" respectively. The current of the HRS reading at -10 V is about 2×10^{-6} μA, which is designated as level "0". The R ratios between two neighboring levels are at least ten times. These results show that the resistive switching memory device fabricated with Sb-doped ZnO has potential application in multilevel resistive memory technology.

The overall resistive switching behavior is controlled by the formation and rupture of Ag nanoisland chain on the nanowire surface [40]. The incorporation of dopants adds additional dimension to the operation of the nanowire resistive memories. Generally, Ga-doping leads to enhanced n-type conduction while Sb-doping results in more resistive or even change of conductivity type from n- to p-type. Although it is clearly demonstrated in the experiments that these dopants play main roles in the formation of self-rectifying or both self-rectifying and self-compliance behavior, how exactly these dopants contribute to the different behavior remains elusive, which needs to be further studied in the future.

Conclusions

Three kinds of resistive switching behavior, i.e. typical bipolar, current self-rectifying, current self-compliance and self-rectifying, were observed in undoped, Ga-doped and Sb-doped ZnO single nanowire devices, respectively. Although the mechanism needs to be further elucidated, this work suggests that the doping of Ga and Sb into ZnO can change the resistive switching behavior and may eventually lead to an RRAM architecture without needing to adopt external selector and current limiter devices.

Acknowledgements

This work was supported in part by the National Natural Science Foundation of China (No. 50902065), Open Project of Key Laboratory for Magnetism and Magnetic Materials of the Ministry of Education, Lanzhou University (LZUMMM2015012), the National Science Foundation for Fostering Talents in Basic Research of the National Natural Science Foundation of China （Nos. 041105 and 041106), and the FAME, one of six centers of STARnet, a Semiconductor Research Corporation program supported by MARCO and DARPA.

References

1 G. W. Burr, B. N. Kurdi, J. C. Scott, C. H. Lam, K. Gopalakrishnan, and R. S. Shenoy, *IMB J. Res. Dev.*, 2008, **52**, 449.
2 Y. Yang, J. Ouyang, L. Ma, R. J. H. Tseng, and C. W Chu, *Adv. Funct. Mater.*, 2006, **16**, 1001.
3 Y. J. Park, L.-S. Bae, S. J. Kang, J. Chang, and C. Park, *IEEE Trans. Dielectr. Electr. Insul.*, 2010, **17**, 1135.
4 J. C. Scott, and L. D. Bozano, *Adv. Mater.* 2007, **19**, 1452.
5 B. Cho, S. Song, Y. Ji, T. W. Kim, and T. Lee, *Adv. Funct. Mater.*, 2011, **21**, 2806.
6 F. Pan, S. Gao, C. Chen, C. Song, F. Zeng, *Mat. Sci. Eng. R.*, 2014, **83**, 1.
7 R. Waser, and M. Aono, *Nat. Mater.*, 2007, **6**, 833.
8 D. H. Kwon, K. M. Kim, J. H. Jang, J. M. Jeon, M. H. Lee, G. H. Kim, X. S. Li, G. S. Park, G. S. Lee, B. Lee, S. Han., M. Kim, and C. S. Hwang, *Nat. Nanotechnol.*, 2010, **5**, 148.
9 Y. Li, D. Qiu, L. Cao, C. Shao, L. Pan, L. Pu, J. Xu, and Y. Shi, *Appl. Phys. Lett.*, 2010, **96**, 133303.
10 S. J. Kang, I.-S. Bae, Y. J. Shin, Y. J. Park, J. Huh, S. M. Park, H. C. Kim, and C. Park, *Nano Lett.*, 2011, **11**, 138.
11 H. Y. Jeong, J. Y. Kim, J. W. Kim, J. O. Hwang, J. E. Kim, J. Y. Lee, T. H. Yoon, B. J. Cho, S. O. Kim, R. S. Ruo, S. Y. Choi, *Nano Lett.*, 2010, **10**, 4381.
12 J. Ouyang, C. W. Chu, C. R. Szmanda, L. Ma, and Y. Yang, *Nat. Mater.*, 2004, **3**, 918.
13 S. P. Heluani, G. Braunstein, M Villafuerte., G. Simonelli, and S. Duhalde, *Thin Solid Films*, 2006, **515**, 2379.
14 Y. Hosoi, Y. Tamai, T. Ohnishi, K. Ishihara, T. Shibuya, Y. Inoue, S. Yamazaki, T. Nakano, S. Ohnishi, N. Awaya, H. Inoue, H. Shima, H. Akinaga, H. Takagi, H. Akoh, and Y. Tokura, *Tech. Dig. Int. Electron Device Meet.*, 2006, **793**, 1.
15 J. Qi, M. Olmedo, J.-G. Zheng, and J. Liu, *Sci. Rep.*, 2013, **3**, 2405.
16 Y. Yang, X. Zhang, M. Gao, F. Zeng, W. Zhou, S. Xie, and F. Pan, *Nanoscale*, 2011, **3**, 1917.
17 N. Xu, L. F. Liu, X. Sun, C. Chen, Y. Wang, D. D. Han, X. Y. Liu, R. Q. Han, J. F. Kang, and B. Yu, *Semicond. Sci. Technol.*, 2008, **23**, 075019.
18 F. Zhuge, S. Peng, C. He, X. Zhu, X. Chen, Y. Liu, and R.-W. Li, *Nanotechnology*, 2011, **22**, 275204.
19 G. Chen, C. Song, C. Chen, S. Gao, F. Zeng, and F. Pan, *Adv. Mater.*, 2012, **24**, 3515.
20 J. Qi, M. Olmedo, J. Ren, N. Zhan, J. Zhao, J.-G. Zheng, and J. Liu, *ACS Nano*, 2012, **6**, 1051.
21 Z. Y. Fan, and J. G. Lu, *IEEE Trans. Nano.*, 2006, **5**, 393.
22 X. Pan, X. Liu, A. Bermak, Z. Fan, *ACS Nano*, 2013, 7, 9318.
23 X. Liu, Y. Long, L. Liao, X. Duan, and Z. Fan, *ACS Nano*, 2012, **6**, 1888.
24 Z. Y. Fan, H. Razavi, J. Do, A. Moriwaki, O. Ergen, Y.-L. Chueh, P. W. Leu, J. C. Ho, T. Takahashi, L. A. Reichertz, S. Neale, K. Yu, M. Wu, J. W. Ager, and A. Javey, *Nat. Mater.*, 2009, **8**, 648.
25 B. Hua, B. Wang, M. Yu, P. W. Leu, and Z. Fan, *Nano Energy*, 2013, **2**, 951.
26 L. Y. Cao, J. S. White, J.-S. Park, J. A. Schuller, B. M. Clemens, and M. L. Brongersma, *Nat. Mater.*, 2009, **8**, 643.
27 P. Kim, L. Shi, A. Majumdar, and P. McEuen, *Phys. Rev. Lett.*, 2001, **87**, 215502.
28 D. Nam, D. S. Sukhdeo, J.-H. Kang, J. Petykiewicz, J. H. Lee, W. S. Jung, J. Vučković, M. L. Brongersma, and K. C. Saraswat, *Nano Lett.*, 2013, **13**, 3118.
29 C. H. Nieh, M. L. Lu, T. M. Weng, and Y. F. Chen, *Appl. Phys. Lett.*, 2014, 104, 213501.
30 S. I. Kim, Y. H. Sa, J.-H. Kim, Y. W. Chang, N. Kim, H. Kim, and K.-H. Yoo, *Appl. Phys. Lett.*, 2014, **104**, 023513.
31 K. Nagashima, T. Yanagida, K. Oka, M. Taniguchi, T. Kawai, J.-S. Kim, and B. H. Park, *Nano Lett.*, 2010, 10, 1359.
32 Z.-M. Liao, C. Hou, Q. Zhao, D.-S. Wang, Y.-D. Li, and D.-P. Yu, *Small*, 2009, **5**, 2377.
33 K. Kim, S. Gaba, D. Wheeler, J. M. Cruz-Albrecht, T. Hussain, N. Srinivasa, W. Lu, *Nano Lett.*, 2012, **12**, 389.
34 J. J. Yang, M. D. Pickett, X. Li, D. A. A. Ohlberg, D. R. Stewart, and R. S. Williams, *Nat. Nanotechnol.*, 2008, **3**, 429.
35 K. Nagashima, T. Yanagida, K. Oka, M. Taniguchi, T. Kawai, J. Kim, and B. H. Park, *Nano. Lett.*, 2010, **10**, 1359.
36 K. Oka, T. Yanagida, K. Nagashima, T. Kawai, J. Kim, and B. H. Park, J. Am. Chem. Soc. 2010, **132**, 6634.
37 J. Kolar, J. M. Macak, K. Terabeb, and T. Wagnera, *J. Mater. Chem. C*, 2014, **2**, 349.
38 Q. Zuo, S. Long, Q. Liu, S. Zhang, Q. Wang, Y. Li, Y. Wang, and M. Liu, *J. Appl. Phys.* 2009, **106**, 073724.
39 S. Balatti, S. Larentis, D. C. Gilmer, and D. Ielmini, *Adv. Mater.*, 2013, **25**, 1474.
40 J. Qi, J. Huang, D. Paul, J. Ren, S. Chu, and J. Liu, *Nanoscale*, 2013, **5**, 2651.